In vitro synthesis of uniform poly(dG)–poly(dC) by Klenow exo⁻ fragment of polymerase I

Alexander B. Kotlyar[1,2,*], Natalia Borovok[1], Tatiana Molotsky[1], Ludmila Fadeev[1,3] and Michael Gozin[3]

[1]Department of Biochemistry, George S. Wise Faculty of Life Sciences, [2]Nanotechnology Center and [3]School of Chemistry, Tel Aviv University, Ramat Aviv, 69978 Israel

ABSTRACT

In this paper, we describe a production procedure of the one-to-one double helical complex of poly(dG)–poly(dC), characterized by a well-defined length (up to 10 kb) and narrow size distribution of molecules. Direct evidence of strands slippage during poly(dG)–poly(dC) synthesis by Klenow exo⁻ fragment of polymerase I is obtained by fluorescence resonance energy transfer (FRET). We show that the polymer extension results in an increase in the separation distance between fluorescent dyes attached to 5′ ends of the strands in time and, as a result, losing communication between the dyes via FRET. Analysis of the products of the early steps of the synthesis by high-performance liquid chromatography and mass spectroscopy suggest that only one nucleotide is added to each of the strand composing poly(dG)–poly(dC) in the elementary step of the polymer extension. We show that proper pairing of a base at the 3′ end of the primer strand with a base in sequence of the template strand is required for initiation of the synthesis. If the 3′ end nucleotide in either poly(dG) or poly(dC) strand is substituted for A, the polymer does not grow. Introduction of the T-nucleotide into the complementary strand to permit pairing with A-nucleotide results in the restoration of the synthesis. The data reported here correspond with a slippage model of replication, which includes the formation of loops on the 3′ ends of both strands composing poly(dG)–poly(dC) and their migration over long-molecular distances (μm) to 5′ ends of the strands.

INTRODUCTION

It has long been known that short-chain deoxyribonucleotides, which contain defined repeating sequences, act as efficient template-primers for the DNA polymerase to provide high-molecular weight double-stranded polymers containing the same repeating nucleotide sequence embodied by the template (1). A series of such polymers has been synthesized with DNA polymerase I of *Escherichia coli* (2–7). High-molecular weight deoxyribopolynucleotides, which contain repeating base sequences, are of interest as model compounds for a variety of chemical and biological studies. The polymers have been well characterized and have been the subject of considerable investigation using biochemical and biophysical methods (8). Most of the deoxyribopolynucleotides were shown to be rigid, double-stranded macromolecules made up of two antiparallel strands held together by hydrogen bonding between complimentary bases. In contrast to poly(dA)–poly(dT) containing equal amounts of A and T bases (2), poly(dG)–poly(dC) is a double-stranded polymer consisting of a pair of poly(dC) and poly(dG) homopolymer chains characterized by unequal content of G and C nucleotides. The ratio of G to C bases was found to vary from 35 to 80% of G (3,9,10). Various approaches have been used to synthesize the polymer (10). Commercial preparations used in 60th and 70th were produced by unprimed (*de novo*) synthesis catalyzed by *E.coli* DNA polymerase in the presence of dGTP and dCTP, as described by Kornberg and co-workers (3). The commercial preparation of dG–dC available at present is manufactured by Amersham Biosciences Company (Sweden) and can be purchased either directly from the company or via Sigma–Aldrich (USA). The commercial preparation is synthesized using the Klenow fragment of DNA polymerase I, dGTP, dCTP and poly(dI)–poly(dC) as the template-primer. The exact procedure of the polymer manufacturing has not been published, and the properties of the synthesis product had not been characterized in detail. The product may contain some single-stranded regions as indicated in the information sheet supplied by the company.

We have been interested in the application of poly(dG)–poly(dC) and its complexes with metal ions in nanoelectronics. As it is regular, poly(dG)–poly(dC) provides the best conditions for π overlap. In addition, guanines, which have the

*To whom correspondence should be addressed. Tel: +972 3 640 7138; Fax: +972 3 640 6834; Email: s2shak@post.tau.ac.il

lowest ionization potential among DNA bases, promote charge migration through the DNA. Recent experimental demonstration of the conducting behavior in short poly(dG)–poly(dC) DNA oligomers (11,12) and the results of theoretical calculations showing that poly(dG)–poly(dC) exhibits better conductance than poly(dA)–poly(dT) (13), support an idea of possible application of poly(dG)–poly(dC) in molecular electronic devices. However, commercial preparations of poly(dG)–poly(dC) used by researchers in electrical conductivity studies (14,15) have a number of disadvantages. They are characterized by a broad size distribution of the molecules and the presence of single-stranded fragments along the DNA. The presence of irregular fragments and strand breaks along poly(dG)–poly(dC) may strongly reduce the ability of the wires to conduct a current. The above disadvantages of the commercial polymer stimulated us to develop a reliable procedure for poly(dG)–poly(dC) production and to study the kinetics and mechanism of its synthesis.

In the present work, we describe a procedure of synthesis of uniform, long (up to 10 kb) double-stranded poly(dG)–poly(dC) composed of G- and C-homopolymers having equal lengths. Direct evidence of strands slippage during extension of template-primer by Klenow exo⁻ fragment of polymerase I from *E.coli* is obtained by fluorescence resonance energy transfer (FRET). Analysis of the products of the early steps of the synthesis by high-performance liquid chromatography (HPLC) and mass spectroscopy suggest that only one nucleotide is added to each of the strand composing poly(dG)–poly(dC) in the elementary step of the polymer extension. A model of poly(dG)–poly(dC) replication, which includes the formation of hairpin loops on 3′ ends of both strands composing the polymer and their migration over long-molecular distances (μm) to 5′ ends of the strands, is discussed.

MATERIALS AND METHODS

Materials

Unless otherwise stated, the reagents were obtained from Sigma–Aldrich (USA) and were used without further purification. The 2′-deoxyribonucleoside 5′-triphosphates (dGTP and dCTP) were purchased from Sigma–Aldrich (USA). Klenow fragment exonuclease minus of DNA polymerase I, *E.coli* lacking the 3′→5′ exonuclease activity (Klenow exo⁻) was purchased from Fermentas (Lithuania).

DNA samples

The oligonucleotides were purchased from Alpha DNA (Montreal, Canada). Fluorescein (Flu) and tetramethylrhodamine (TAMRA) labeled oligonucleotides were also from Alpha DNA (Canada). The Flu and TAMRA were linked to the terminal base at the 5′ end of G-12mer $(dG)_{12}$ and C-12mer $(dC)_{12}$ oligonucleotides, respectively, via a six-carbon linker. The nomenclatures used for the above oligonucleotides are as follows: Flu-$(dG)_{12}$ and TAMRA-$(dC)_{12}$. Poly(dC)-oligonucleotides were purified using an ion-exchange Western Analytical Products (USA) PolyWax LP column (4.6 × 200 mm, 5 μm, 300 Å) at pH 7.5. Poly(dG)-oligonucleotides were purified using a ion-exchange HiTrap QHP column (5 × 1 ml) from Amersham-Biosciences (Sweden) in 0.1 M KOH. The dye-labeled probes were purified by

HPLC using a Vydac (USA) reverse-phase C_{18} column (4.6 × 250 mm). HPLC-purified oligonucleotides were desalted using pre-packed Sephadex G-25 DNA-Grade columns (Amersham-Biosciences). Purified oligomers were incubated with their complementary counterparts in 0.1 M KOH at a molar ratio of 1:1 for 15 min and dialyzed against 20 mM Tris–Acetate buffer, pH 7.0, for 4 h. All oligonucleotides were quantified spectrophotometrically using their respective extinction coefficients. Concentrations of G- and C-homopolymers were calculated using extinction coefficients at 260 nm of 11.7 and 7.5 mM⁻¹ cm⁻¹ for G and C bases. CD spectra of poly(dG)–poly(dC) were measured on Aviv Model 202 series (Aviv Instrument Inc., USA) Circular Dichroism Spectrometer. Each spectrum was recorded from 220 to 340 nm and was an average of five measurements.

DNA polymerase assays

A standard reaction contained 60 mM KPi, pH 7.4, 5 mM $MgCl_2$, 5 mM DTT, and 1.5 mM each of dCTP and dGTP, the Klenow exo⁻ and the template-primer. The concentration and the nature of template-primer and concentration of Klenow exo⁻ are noted in the figure legends. The reaction was started by the addition of the enzyme. The incubation was at room temperature (25°C) or at 37°C for the times indicated in the figure legends. The reaction was terminated by the addition of EDTA to a final concentration of 10 mM. Reaction products were analyzed by size exclusion and ion-exchange HPLC, as well as by electrophoresis on an agarose gel.

HPLC separation of the polymerase products

Poly(dG)–Poly(dC) were separated from nucleotides, template-primer and other reaction components of the synthesis using size-exclusion HPLC. The separation was achieved with a TSK-gel G-DNA-PW HPLC column (7.8 × 300 mm) from TosoHaas (Japan) by isocratic elution with 20 mM Tris–Acetate, pH 7.0, for 30 min at a flow rate of 0.5 ml/min. Size-dependent separation of the strands composing poly(dG)–poly(dC) was performed using the same column by isocratic elution with 0.1 M KOH at a flow rate of 0.5 ml/min. The injection volumes were 50–200 μl. All experiments were conducted on an Agilent 1100 HPLC system with a photodiode array detector. Peaks were identified from their retention times obtained from the absorbance at 260 nm. Data were collected from PDA and analyzed by Microsoft Excel.

Separation of 10–18 bp long G- and C-homopolymers originating from the early polymerase synthesis was performed using ion-exchange TSKgel DNA-NPR column (4.6 × 75 mm) from Tosoh Biosciences (Japan) at a high-pH. The oligonucleotides were eluted with a linear gradient of KCl from 0 to 1 M in 0.1 M KOH at a flow rate of 0.6 ml/min. Ion-exchange HPLC was also used as a method to determine the concentrations of dGTP and dCTP nucleotides in the assay. HPLC separation of the dNTPs was performed with an ion-exchange PolyWax LP HPLC column (4.6 × 200 mm, 5 μm, 300 Å) from Western Analytical (USA), using a linear gradient of 20–500 mM potassium phosphate buffer, pH 7.4.

Gel electrophoresis

The products of polymerase synthesis and commercial preparations of poly(dG)–poly(dC) were loaded onto 1% agarose gel

and then electrophoresed at room temperature at 130 V for 1 h. TAE buffer, in addition to being used to prepare the agarose, also served as the running buffer. The dimensions of the agarose gel were 10×10 cm with 2×4 mm 14-wells. The gel was stained with ethidium bromide (5 µg/ml) and visualized with a Bio Imaging System 202D (302 nm).

FRET measurements

Extension of fluorescently labeled oligonucleotides were performed in 100 mM Tris–Acetate, pH 8.0, 3 mM $MgCl_2$, 5 mM DTT, and 1 mM each of dCTP and dGTP, 0.8 µg/ml of Klenow exo$^-$ and 5 µM Flu-$(dG)_{12}$–TAMRA-$(dC)_{12}$ duplex. The steady-state fluorescence measurements were done with Model LS50B Perkin-Elmer (UK) Luminescence Spectrometer. Excitation was at 490 nm with emission at 520 nm. The slits for excitation and emission monochromators were both set at 2.5 nm.

Absorption spectra of the synthesized products were recorded with U2000 Hitachi (Japan) spectrophotometer. The contents of Flu, TAMRA and G–C base pairs were estimated using the following extinction coefficients: $\varepsilon^{Flu}(494\ nm) = 77\,000\ M^{-1}\ cm^{-1}$, $\varepsilon^{TAMRA}(558\ nm) = 90\,000\ M^{-1}\ cm^{-1}$ (16), $\varepsilon^{GC}\ (260\ nm) = 14\,800\ M^{-1}\ cm^{-1}$ (4). The contributions of the dyes to absorption at 260 nm were calculated based on their concentrations and their extinction coefficients, $\varepsilon^{Flu} = 20\,900\ M^{-1}\ cm^{-1}$ and $\varepsilon^{TAMRA} = 31\,900\ M^{-1}\ cm^{-1}$ at 260 nm. The contribution of the dye at 260 nm was subtracted and the concentration of G–C pairs in each sample of synthesized poly(dG)–poly(dC) was then determined.

Mass spectrometer conditions

Mass spectrometric measurements of oligonucleotides were carried out on a Finnigan LCQ Classic ion trap instrument (ThermoFinnigan, San Jose, CA) equipped with its standard heated capillary electrospray source. The source was operated in the negative ion mode, with a heated capillary temperature normally set at 150°C and needle voltage at −3 kV (17). Mass spectra were recorded in a row scan mode in the mass range from m/z of 500 to 2000. All mass spectra were obtained by signal averaging for 1 min at a scan rate of 3 microscans/scan. Solutions of oligonucleotides were admitted by direct infusion with a 100 µl Hamilton gas-tight syringe (Holliston, MA) at a flow rate of 3 µl/min. Typical 1 µM solution of oligonucleotide was injected into 25 mM triethylamine (TEA), 25 mM hexafluoroisopropanol (HFIP) and 50% acetonitrile.

RESULTS

Synthesis and characterization of poly(dG)–poly(dC)

Electrophoresis analysis of poly(dG)–poly(dC) preparations purchased from Sigma and synthesized here by Klenow exo$^-$, in a non-denaturing agarose gel (described in Materials and Methods), is shown in Figure 1. As seen in Figure 1, the commercial preparation does not enter the gel (lane 2). This might be due to the aggregation of the DNA molecules. Heating the preparation for 30 min at 70°C did not result in the dissociation of the aggregates. A small fraction of the molecules that enters the gel after the heat treatment is
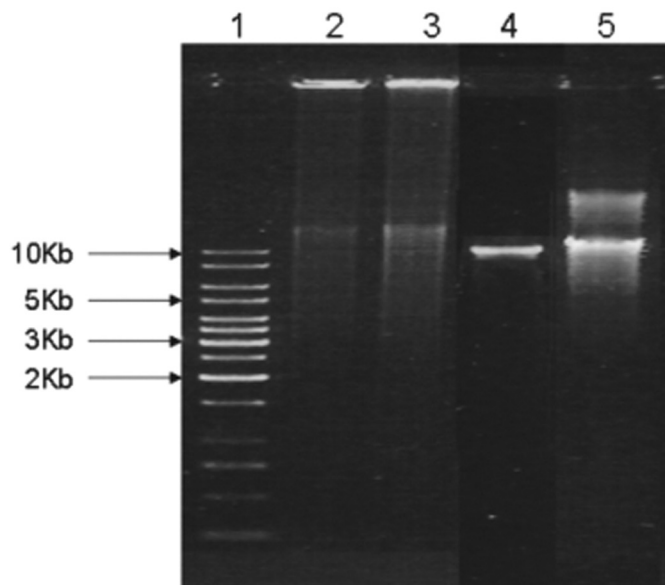

Figure 1. Mobility of poly(dG)–poly(dC) molecules in 1% agarose gel. Electrophoresis of the molecules: molecular weights of 1 kb DNA-ladder (lane 1) are indicated by left-hand side narrows; poly(dG)–poly(dC) from Sigma, lot 103K10561 (lane 2); poly(dG)–poly(dC) from Sigma treated for 30 min at 70°C (lane 3); poly(dG)–poly(dC) synthesized as described in Materials and Methods using HPLC-purified 0.2 µM $(dG)_{10}$–$(dC)_{10}$ as template-primer and 40 µg/ml of Klenow exo$^-$ (lane 4); poly(dG)–poly(dC) synthesized as described in Materials and Methods using 0.2 µM $(dG)_{10}$–$(dC)_{10}$ not specially purified by HPLC as template-primer and 40 µg/ml of Klenow exo$^-$ (lane 5). The electrophoresis was conducted for 1 h at 130 V. The amount of DNA loaded per lane was ∼20 ng and the gel was ethidium bromide stained.

characterized by a broad distribution of molecular sizes and shows a smeared band pattern (Figure 1, lane 3). In contrast to the commercial polymer, poly(dG)–poly(dC) synthesized here had no problem entering the gel and was characterized by a narrow distribution of molecular sizes (Figure 1, lane 4). We performed an analysis of strands, which compose the commercial and synthesized polymers by size exclusion HPLC, at high-pH. At pH > 12.5, the poly(dG) and the poly(dC) strands are being separated. As seen in Figure 2 (solid line), poly(dG)–poly(dC) synthesized here (see Materials and Methods) is also eluted as a single peak from the column at high-pH, thus proving that G- and C-strands, which compose the polymer, are equal in size. Elution profile of the commercial polymer is different from the synthesized one and is presented by two overlapped peaks (see Figure 2, dashed line). Absorption spectroscopy analysis of the eluted fraction showed that the earlier peak eluted between 13 and 16.5 min is characterized by a spectrum of C-homopolymer, while the peak eluted between 17 and 22 min has a spectrum of G-homopolymer (see insets in Figure 2). Different retention times of C- and G-strands are indicative of the different lengths of the strands composing the commercial polymer. C-strand of the commercial polymer is eluted from the column in a volume similar to that of the 7 kb poly(dG)–poly(dC) (see Figure 2). The G-strand is eluted in a volume corresponding to that of 1.5 kb DNA (data not shown). The above analysis clearly shows that the G-strand composed of poly(dG)–poly(dC) obtained from Sigma is about five times shorter than the corresponding C-strand. Thus, the commercial preparation can hardly be

considered as a double-stranded poly(dG)–poly(dC), comprising of two consecutive G- and C-homopolymer strands.

We describe below a procedure of production of a long (up to 10 kb) uniform poly(dG)–poly(dC) composed of the one-to-one double helical complex of polydeoxyguanylate and polydeoxycytidylate. Poly(dG)–poly(dC) was synthesized here by Klenow exo$^-$ fragment of DNA polymerase I in the presence of dGTP, dCTP and (dG)$_{10}$–(dC)$_{10}$ oligonucleotides. We have shown that, if primed by non-purified (dG)$_{10}$–(dC)$_{10}$, the synthesis yielded polymer molecules with large length variability (Figure 1, lane 5). The (dG)$_{10}$–(dC)$_{10}$ prepared from HPLC purified (dG)$_{10}$ and (dC)$_{10}$, as described in Materials and Methods, primes synthesis of uniform poly(dG)–poly(dC) (see Figure 1, lane 4).
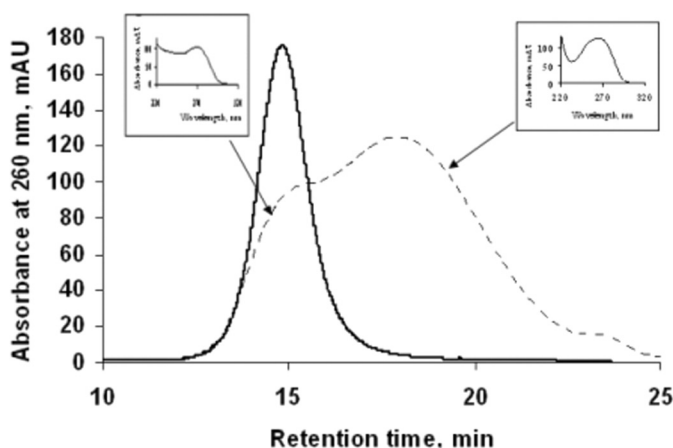

Figure 2. Size-dependent HPLC of poly(dG)–poly(dC) at high-pH. Poly(dG)–poly(dC) synthesized with Klenow exo$^-$ as described in Figure 1 (solid curve) and poly(dG)–poly(dC) from Sigma (dashed curve) were pretreated for 15 min at room temperature in 0.1 M KOH. A total of 100 μl of each DNA sample were applied onto TSKgel G-DNA-PW column (7.8 × 300 mm) and eluted at room temperature with 0.1 M KOH at a flow rate of 0.5 ml/min. The length of the synthesized poly(dG)–poly(dC) estimated by gel electrophoresis as shown in Figure 1 is equal to 7 kb. Elution was followed at 260 nm. Insets present normalized absorbance spectra obtained using diode-array detection of fractions eluted at the time points indicated by the arrows.

We have shown that (dG)$_{30}$–(dC)$_{30}$ can also efficiently prime synthesis of long poly(dG)–poly(dC), supporting the earlier observation of Rao and co-workers (18). However, this synthesis never yielded uniform poly(dG)–poly(dC), regardless of whether the oligonucleotides composing the template-primer were purified by HPLC or not. This might be due to the formation of kinetically stable structures with overhangs when 30 base (or longer) poly(dG) and poly(dC) oligonucleotides are used to form a double-stranded template-primer. We have shown that, when primed by overhangs containing, (dG)$_{12}$–(dC)$_{15}$ and (dG)$_{15}$–(dC)$_{12}$ duplexes, the synthesis yielded various lengths of poly(dG)–poly(dC) (data not shown), thus supporting the above suggestion. Overhangs containing temporary structures, even if formed while annealing of (dG)$_{10}$ and (dC)$_{10}$, are spontaneously and rapidly rearranged (at 37°C) into more stable, completely annealed (dG)$_{10}$–(dC)$_{10}$ duplexes that prime synthesis of uniform poly(dG)–poly(dC).

Kinetics of poly(dG)–poly(dC) synthesis primed by HPLC purified (dG)$_{10}$–(dC)$_{10}$ is depicted in Figure 3. The molecules grew continuously until the dGTP and dCTP were exhausted. Analysis of the data reveals a linear dependence of the polymer length on the time of the synthesis (see Figure 3B). Thus, the rate of polymer growth is independent of the length of the fragments being synthesized. The reaction product can be purified and used as a template-primer for a further synthesis. We have observed that hundreds of base pairs of poly(dG)–poly(dC) started to grow again, leading to thousands of base pair long uniform molecules (data not shown).

A ratio of G to C nucleotides in poly(dG)–poly(dC) preparations reported in the literature was strongly dependent on the synthesis conditions (10). For conclusion of the content of dG and dC bases in poly(dG)–poly(dC), we estimated the amount of the nucleotides consumed during the synthesis of the polymer. The reaction was conducted as described in Figure 3 for 150 min and was arrested by adding EDTA to the assay mixture. The products of the synthesis were separated from dGTP and dCTP by size-exclusion HPLC (see Figure 4A). As shown in the figure, incubation of Klenow exo$^-$ with dGTP, dCTP and (dG)$_{10}$–(dC)$_{10}$ results in the appearance of a peak
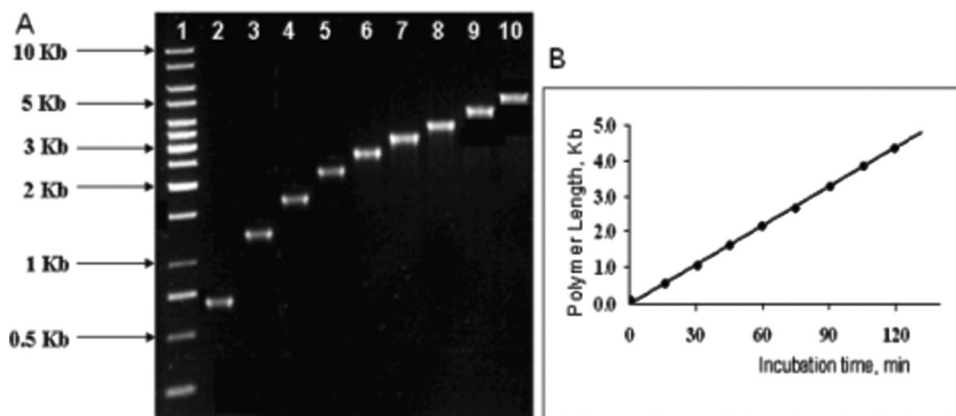
Figure 3. Time course of poly(dG)–poly(dC) synthesis reaction. Polymerase extension assay was performed as described in Materials and Methods with 0.2 μM (dG)$_{10}$–(dC)$_{10}$ and 20 μg/ml of Klenow exo$^-$; the incubation was at 37°C. Aliquots were withdrawn each 15 min for 2 h 15 min. (**A**) The reaction products were resolved on 1% agarose gel and stained with ethidium bromide under conditions described in Materials and Methods. The marker bands of 1 kb DNA ladder (lane 1) are indicated to the left. Time-dependent products for 15, 30, 45, 60, 75, 90, 105, 120 and 135 min of the synthesis (lanes 2–10). (**B**) Dependence of the polymer length (in kb) estimated from (A) on the time of synthesis.
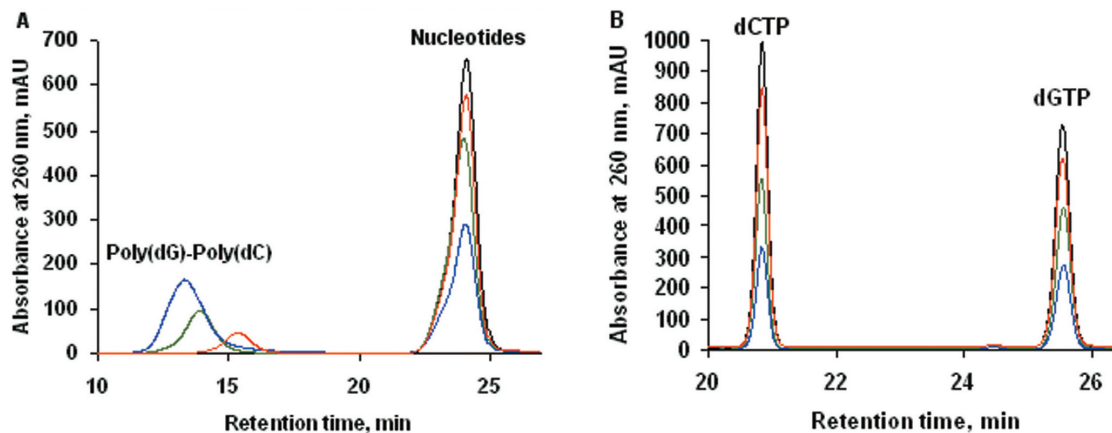
Figure 4. HPLC analysis of nucleotides incorporation into poly(dG)–poly(dC). (**A**) Size-dependent HPLC separation of the products of polymerase synthesis. Polymerase extension assay was performed as described in Materials and Methods with 0.2 μM $(dG)_{10}$–$(dC)_{10}$ and 20 μg/ml of Klenow exo⁻ at 37°C. Polymerization reaction was started by addition of the enzyme. Aliquots of 50 μl were withdrawn from the assay mixture before (black curve) and 30 (red curve), 60 (green curve) and 120 (blue curve) min after the addition of the enzyme and loaded on TSKgel G-DNA-PW column (7.8 × 300 mm). Elution was performed with 20 mM Tris–Acetate buffer, pH 7.0, at a flow rate of 0.5 ml/min. (**B**) Anion-exchange HPLC separation of nucleotides. Nucleotide peaks from corresponding size-exclusion separation (A) were collected and loaded on an anion-exchange PolyWax LP column (4.6 × 200 mm). Elution was performed using a 30 min linear K-Pi, pH 7.4, gradient between 0.02 and 0.5 M in the presence of 10% acetonitrile at a flow rate of 0.8 ml/min. Elution was followed at 260 nm.

Table 1. Incorporation of deoxyribonucleosine triphosphates into poly(dG)–poly(dC)

Time of synthesis (min)	dGTP (nmol)	dCTP (nmol)
0	18.3	18.4
30	15.8	16.1
60	10.5	11.0
120	8.6	8.5
150	6.3	6.4

The values were estimated as shown in Figure 4. All values are averages of five measurements.

eluted before total column volume. This peak corresponds with a high-molecular weight poly(dG)–poly(dC) product of the synthesis. Its position shifts left and its height grows (see Figure 4A) as the synthesis progresses. The peak eluted from the column in total volume comprises a mixture of dGTP and dCTP. A height of the latter peak decreases along with the increase of the poly(dG)–poly(dC) peak (see Figure 4A), which corresponds with incorporation of the nucleotides into the polymer. The peak eluted with total volume was collected and the amounts of dGTP and dCTP in the peak were estimated. The dGTP and dCTP were separated one from another by ion-exchange HPLC as shown in Figure 4B. The first peak eluted from the ion-exchange column corresponds to dCTP and the second one to dGTP. Both peaks were collected separately and the quantities of the nucleotides were estimated by spectrophotometer; 7.5×10^3 and 11.7×10^3 M^{-1} cm^{-1} extinctions coefficient at 260 nm were used for dCTP and dGTP, respectively. The results of this analysis are summarized in Table 1. As evident from Table 1, equal amounts of dCTP and dGTP have been consumed from the assay during the synthesis of the polymer. Thus, the data presented in Figures 2 and 4 suggest that the procedure described herein results in the formation of one-to-one double helical complex of polydeoxyguanylate and polydeoxycytidylate.

Additional evidences for the double-stranded nature of synthesized poly(dG)–poly(dC) are derived from the digestion experiments of the polymer with Deoxyribonuclease I (DNase) and from the CD spectroscopy. We have shown that DNase efficiently digests poly(dG)–poly(dC) to short oligonucleotides. The enzyme is specific with respect to double-stranded DNA; thus, digestion by the enzyme is reflective of the double-stranded nature of the polymer. The major characteristics of CD spectrum of poly(dG)–poly(dC), namely, a positive band at 235 nm, a crossover at 244, and negative band at 235 nm, are similar to those reported for double-stranded poly(dG)–poly(dC) earlier (10).

Poly(dG)–poly(dC), if exposed to high-pH for 5–10 min and subsequently neutralized, undergoes irreversible rearrangement into a mixture of C- and G-containing polymers. The alkali-treated polymer behaves differently on size-exclusion HPLC, electrophoresis, is inert with respect to DNase and is characterized by different optical and CD spectra compared to a non-treated polymer. Irreversible changes in poly(dG)–poly(dC) at high-pH are mainly due to the fact that both G- and C-strands that compose the polymer have a tendency to form stable intramolecular and intermolecular homopolymer structures namely, double-stranded poly(dC):(dC+) (10,19,20) and poly(dG) quadruplexes (21,22).

FRET studies of poly(dG)–poly(dC) extension

The effect of modifications on the ability of $(dG)_{12}$–$(dC)_{12}$ to prime the synthesis of poly(dG)–poly(dC) is summarized in Table 2. The data presented in the Table show that either covalent modification of one of 3′ ends of $(dG)_{12}$–$(dC)_{12}$ or substitution of C or (and) G at the 3′ end(s) of the oligonucleotide with A-nucleotide, results in the complete loss of the ability of the oligonucleotide to prime the synthesis. In contrast, covalent modification of the 5′ ends or replacement of either C or G bases at the 5′ ends with A-nucleotide, have no effect on the capacity of the oligonucleotide to prime the

synthesis. The latter enabled us to study the dynamics of the polymerase synthesis by FRET using $(dG)_{12}–(dC)_{12}$ labeled at the 5′ ends with different fluorescent dyes. FRET is an important technique for investigating a variety of biological phenomena that produce changes in molecular proximity. The approach proved to be very useful for studies of DNA and RNA structures and the interaction of nucleic acids with proteins (23,24). In FRET, a donor fluorophore is excited by incident light, and if an acceptor is in close proximity, the excited state energy from the donor is transferred by means of intermolecular long-range dipole–dipole coupling (25). The efficiency of FRET is dependent on the inverse sixth power of the intermolecular separation of the donor. Thus, FRET provides a sensitive measure of small changes in intermolecular distances. Flu energy donor and TAMRA energy acceptor moieties meet spectroscopic criteria, important in a study of energy transfer (26). The above dyes were employed in this work to monitor dynamics of the primer-template extension by the polymerase. The $(dC)_{12}$ and $(dG)_{12}$ oligonucleotides labeled at the 5′ ends with TAMRA and Flu, respectively, were used in the FRET experiments. The oligonucleotides were purified by

HPLC and annealed as described in Materials and Methods. Emission of Flu in the $(dG)_{12}–(dC)_{12}$ oligonucleotide labeled at the opposite 5′ ends with Flu and TAMRA is strongly quenched compared to that of the Flu-$(dG)_{12}$. We have shown that quenching is independent of concentration of the $(dG)_{12}–(dC)_{12}$ oligonucleotide, thus supporting the intramolecular mechanism of excitation energy transfer from Flu to TAMRA. Addition of Klenow exo$^-$ to the assay mixture containing Flu-$(dG)_{12}–(dC)_{12}$-TAMRA, dGTP and dCTP caused the increase of Flu emission in time (see Figure 5A). Aliquots were withdrawn from the assay at a different time and the products of the synthesis were analyzed by absorption spectroscopy. Spectra of the oligonucleotide and products of 5, 10, 20, 30, and 40 min synthesis are shown in Figure 5B. Peaks at 565, 496 and 260 nm (see Figure 5B) are attributed to TAMRA, Flu and DNA, respectively. The peak at 260 nm is mainly due to the absorption of the oligonucleotide, whereas contribution of both the dyes to the absorption at 260 nm is minimal. Using extinction coefficient of 14.8×10^3 M^{-1} cm^{-1} for a G–C base pair at 260 nm, we calculated an average number of base pairs in the products of

Table 2. Priming of poly(dG)–poly(dC) synthesis with various double-stranded synthetic DNA sequences

Oligonucleotide	Priming of poly(dG)–poly(dC) synthesis
5′-GGGGGGGGGGGGG**A**-3′–5′-CCCCCCCCCCCCC**A**-3′	No
5′-**A**GGGGGGGGGGGGG-3′–5′**A**CCCCCCCCCCCCC-3′	Yes
5′-GGGGGGGGGGGGG**A**-3′–5′-CCCCCCCCCCCCCC-3′	No
5′-GGGGGGGGGGGGGG-3′–5′-**A**CCCCCCCCCCCCC-3′	Yes
5′-GGGGGGGGGGGGGG-3′–5′-CCCCCCCCCCCCC**A**-3′	No
5′-**A**GGGGGGGGGGGGG-3′–5′-CCCCCCCCCCCCCC-3′	Yes
5′-**Flu**-GGGGGGGGGGGGG-3′–5′-**TAMRA**CCCCCCCCCCCCCC-3′	Yes
5′-**NH$_2$**-GGGGGGGGGGGGG-3′–5′-**NH$_2$**-CCCCCCCCCCCCCC-3′	Yes
5′-GGGGGGGGGGGGG-**NH$_2$**-3′–5′-**CCCCCCCCCCCCCC-NH$_2$-3′**	No
5′-**SH**-GGGGGGGGGGGGG-3′–5′-**SH**-CCCCCCCCCCCCCC-3′	Yes

Reactions were performed as described in Materials and Methods with 5 µM of template-primers and 10 µg/ml of Klenow exo$^-$. The products of synthesis were analyzed by electrophoresis as in Figure 3.
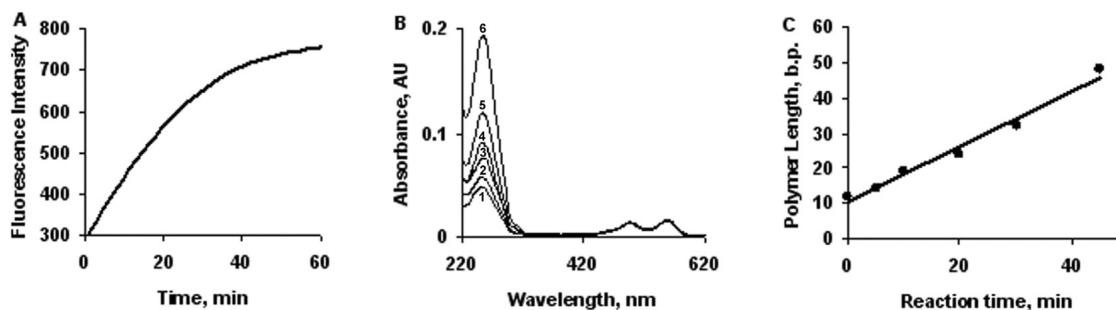
Figure 5. FRET in Flu-$(dG)_{12}–(dC)_{12}$-TAMRA during extension by Klenow exo$^-$. (**A**) Time course of Flu emission. Polymerase extension assay was performed as described in Materials and Methods with 5 µM Flu-$(dG)_{12}–(dC)_{12}$-TAMRA and 0.8 µg/ml of Klenow exo$^-$. The assay mixture containing Flu-$(dG)_{12}–(dC)_{12}$-TAMRA and nucleotides was transferred into a fluorimetric cuvette. Fluorescence emission at 520 nm was recorded in time as described in Materials and Methods; excitation was at 490 nm. A significant amount of energy transfer is detected as a large decrease in the contribution of the Flu donor and an increase in the contribution of the TAMRA acceptor. The extension reaction was started by addition of the enzyme and fluorescence was recorded in time. (**B**) Aliquots of 0.5 ml of sample was withdrawn from the incubation before (curve 1) and 5 (curve 2), 10 (curve 3), 20 (curve 4), 30 (curve 5), and 40 (curve 6) min after addition of the enzyme to the assay. The samples were passed through Sephadex G-25 DNA-Grade column (1 × 5 cm) in 20 mM Tris–Acetate buffer, pH 8.0, to separate high-molecular weight products of the synthesis from nucleotides; absorption spectra of the synthesized polymer eluted in the column's void volume were recorded. (**C**) The amount of G–C base pairs in double-labeled product of the synthesis were estimated from analysis of the spectra presented in (**B**) as described in Materials and Method, and plotted as a function of time of synthesis.
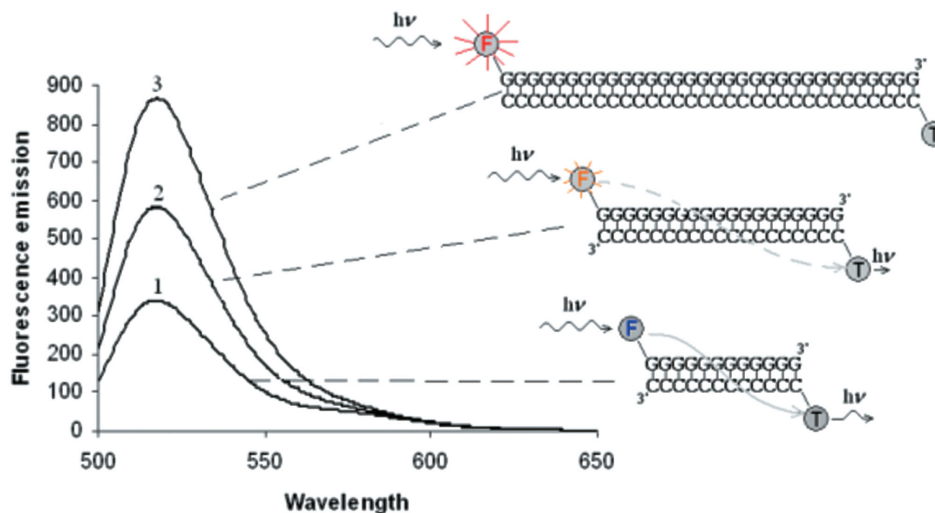
Figure 6. Fluorescence emission spectra of the products of Flu-$(dC)_{12}$–$(dG)_{12}$-TAMRA extension. Polymerase extension assay was performed as described in Figure 5. The spectra were recorded before (curve 1), and 10 (curve 2) and 25 (curve 3) min after initiation of the synthesis. Excitation was at 490 nm. Schematic presentation of corresponding double-stranded products of the synthesis, are indicated to the right; F denotes for Flu, T for TAMRA. A significant amount of energy transfer in Flu-$(dC)_{12}$–$(dG)_{12}$-TAMRA is apparent as a decrease in the contribution of the Flu donor and an increase in the contribution of the TAMRA acceptor. The latter is seen as an increased relative emission around 580 nm in spectra of Flu-$(dC)_{12}$–$(dG)_{12}$-TAMRA. Extension of Flu-$(dC)_{12}$–$(dG)_{12}$-TAMRA results in an increase of molecular distance between the dyes and, as a result, in increase of Flu emission. When the length of extended polymer reaches ∼20 bp (see Figure 5), a reduced amount of energy transfer is apparent (spectrum 2). Flu emission reaches maximum, when the length of extended polymer is equal to ∼30 bp (∼10 nm); no contribution of TAMRA emission is then seen.

the synthesis. The dependence of the calculated length of poly(dG)–poly(dC) on the time of synthesis is shown in Figure 5C. Fluorescence emission spectra of the products of Flu-$(dG)_{12}$–$(dC)_{12}$-TAMRA extension are presented in Figure 6, together with a schematic presentation of the structures of the double-labeled products of the extension. As shown in the figure, energy transfer between the dyes attached at both sides of the template-primer is apparent as a decrease in the contribution of the Flu donor and an increase in the relative contribution of the TAMRA acceptor. The extension results in an increase in the separation distance between the 5′ ends of the strands and in loss of the ability of Flu and TAMRA to communicate via FRET. When the length of the extended polymer reaches ∼30 bp (see Figures 5 and 6), no communication of the dyes is seen and Flu emission reaches a maximum. The latter is in good agreement with the FRET theory, saying that no energy transfer can be observed at distances >100 Å (25). The data of FRET analysis presented in Figures 5 and 6 clearly show that the 5′ ends are moving in opposite directions during extension of the template-primer by Klenow exo⁻.

The early synthesis products of $(dG)_{10}$–$(dC)_{10}$ extension

To investigate the mechanism of synthesis in more detail, we have analyzed the early synthesis products by a combination of HPLC and mass spectroscopy as described in Materials and Methods. The synthesis was conducted for 5 min at 37°C in the presence of small amounts of Klenow exo⁻, dGTP, dCTP and $(dG)_{10}$–$(dC)_{10}$. Products of the synthesis were separated from the nucleotides and passed through the ion-exchange HPLC column at a high-pH as described in Figure 7. Anion-exchange HPLC at high-pH enables the separation of G- and C-strands composing the template-primer. G-bases undergo complete deprotonation at a pH > 12 and an additional negative charge
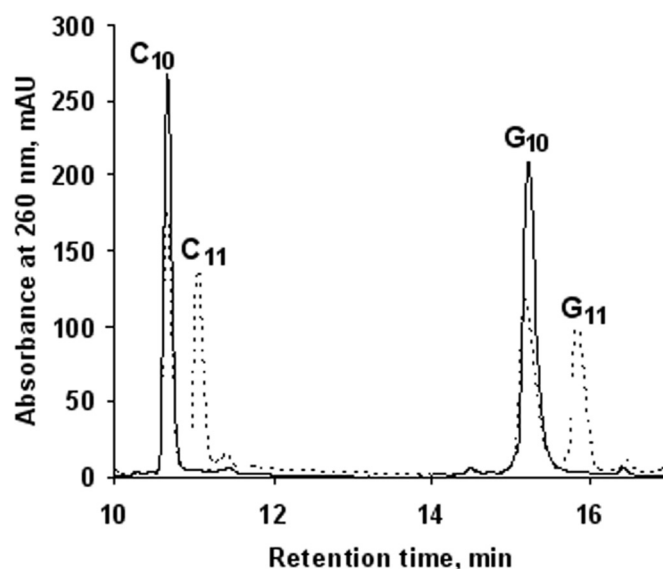
Figure 7. HPLC analysis of products of early phase of poly(dG)–poly(dC) synthesis. Polymerase extension assay was performed as described in Materials and Methods, with 15 µM $(dG)_{10}$–$(dC)_{10}$ and 2 µg/ml of Klenow exo⁻ at 37°C. The reaction was started by addition of the enzyme and was terminated by addition of 10 mM EDTA. Aliquots of 50 µl were withdrawn from the assay mixture before (continuous curve) and 5 min (dashed curve) after the reaction had been started. Oligonucleotides were separated from dGTP and dCTP with TSKgel G-3000 SWXL HPLC column (7.8 × 300 mm) and loaded in 0.1 M KOH onto TSKgel DNA-NPR column (4.6 × 75 mm) equilibrated with 0.1 M KOH. Elution was performed using a 30 min linear KCl gradient between 0 and 1 M in 0.1 M KOH at a flow rate of 0.6 ml/min. Elution of correspondent C- and G-strands are indicated in the figure.

is introduced to each base of G-strand. Higher negative charge of G-strand compared to the corresponding C-strand results in a tighter binding of the G-strand to a positively charged matrix of the column, and as a result, in its elution from the column

**Table 3.** Extension rates for the different template-primer sequences by Klenow exo$^-$

Template-primer	Product of extension	TN (min^{-1})
5′-GGGGGGGGGGG3′–5′CCCCCCCCCCC-3′	5′-GGGGGGGGGGGG-3′–5′-CCCCCCCCCCC-3′	60
5′-GGTGGGGGGGGGA-3′–5′-CCCCCCCCCCCCA-3′	5′-GGTGGGGGGGGGA-3′–5′-CCCCCCCCCCCCACC-3′	50
5′-GGGTGGGGGGGGA-3′–5′-CCCCCCCCCCCCA-3′	5′-GGGTGGGGGGGGA-3′–5′-CCCCCCCCCCCCACCC-3′	20
5′-GGGGTGGGGGGGA-3′–5′-CCCCCCCCCCCCA-3′	5′-GGGGTGGGGGGGA-3′–5′-CCCCCCCCCCCCACCCC-3′	5.6
5′-GGGGGTGGGGGGA-3′–5′-CCCCCCCCCCCCA-3′	5′-GGGGGTGGGGGGA-3′–5′-CCCCCCCCCCCCACCCCC-3′	0.3

The reactions were performed and the rates were determined as described in the legend to Figure 8. The rates are expressed in a number of the enzyme's turnovers per minute.

at higher salt concentrations. Figure 7 presents data of ion exchange HPLC of (dG)$_{10}$–(dC)$_{10}$ (continuous curve) and products of 5 min synthesis (dashed curve). Molecular masses of oligonucleotides composing the template-primer and eluted in the first and second peaks (solid curve) have been estimated by mass spectroscopy (see Materials and Methods) to be equal to 2868 and 3228 D. The estimated masses correspond well with (dC)$_{10}$ and (dG)$_{10}$. Incubation of (dG)$_{10}$–(dC)$_{10}$ with Klenow exo$^-$, dGTP and dCTP for 5 min results in the appearance of two new peaks on the chromatogram to the right of (dC)$_{10}$ and (dG)$_{10}$ ones (Figure 7, dashed curve). Molecular masses of oligonucleotides eluted in the new peaks are equal to 3117 and 3558 D, which correspond with masses of (dC)$_{11}$ and (dG)$_{11}$. These data demonstrate that an elementary step of (dG)$_{10}$–(dC)$_{10}$ extension includes the addition of one base to each of the strands composing the oligonucleotide. As shown in Figure 7 (dashed curve), incubation for 5 min of 15 µM (dG)$_{10}$–(dC)$_{10}$ with 2 µM Klenow exo$^-$ at 37°C results in the conversion of ∼45% of the oligonucleotide to the product. Based on these data, a turnover number of 60 min-1 for Klenow exo$^-$ in the reaction of (dG)$_{10}$–(dC)$_{10}$ was calculated (see Table 3).

Replication of 5′-CCCCCCCCCCCCA-3′–5′-GGGGTGGGGGGGA-3′ and similar oligonucleotides

We have shown (see Table 2) that the replacement of C or G, even at one of the 3′ ends of (dG)$_{12}$–(dC)$_{12}$ with A-nucleotide, results in the complete loss of the ability of the oligonucleotide to prime the synthesis. A reason for that might be the inability of the enzyme to properly pair the A-nucleotide at the 3′ end if no T-nucleotides are present in the sequence of the complimentary strand. Indeed, when T-nucleotide was introduced into a sequence of the strand, replication was restored. Expansion of the double-stranded 5′-CCCCCCCCCCCCA-3′–5′-GGGGTGG-GGGGGA-3′ by Klenow exo$^-$ is demonstrated in Figure 8. Strands composing the oligonucleotide were purified to homogeneity by HPLC, and annealed as described in Materials and Methods. As seen in the Figure, the incubation of 5′-CCCC-CCCCCCCA-3′–5′-GGGGTGGGGGGGA-3′ with Klenow exo$^-$, dGTP and dCTP results in the extension of 5′-CCCC-CCCCCCCA-3′-strand. This is seen as a shift of the peak corresponding to 5′-CCCCCCCCCCCCA-3′ on the chromatogram (see Figure 8, red and blue curves). The position of the second peak, corresponding to 5′-GGGGTGGGGGGGA-3′, remains unchanged. Molecular mass of the oligonucleotide eluted in the shifted peak has been estimated by mass spectroscopy (see Materials and Methods) to be equal to 4876 D. This
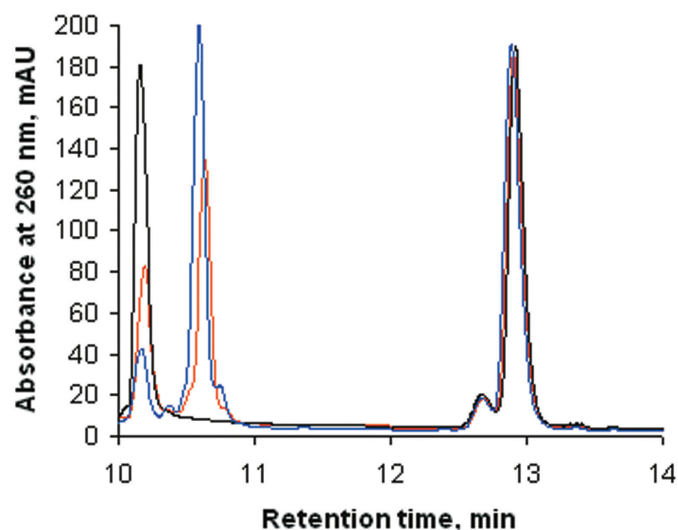
Figure 8. HPLC analysis of products of 5′-CCCCCCCCCCCCA-3′–5′-GGGGTGGGGGGGA-3′ extension. Polymerase extension assay was performed as described in Materials and Methods with 5 µM 5′-CCCCCCCCCCCCA-3′–5′-GGGGTGGGGGGGA-3′ and 10 µg/ml of Klenow exo$^-$ at 37°C. The reaction was started by addition of the enzyme and terminated by addition of 10 mM EDTA. Aliquots of 50 µl of sample were withdrawn from the assay mixture before (black curve) and 10 (red curve), and 20 (blue curve) min after the reaction had been started. Oligomers were separated from dGTP and dCTP with TSKgel G-3000 SWXL HPLC column (7.8 × 300 mm) and loaded in 0.1 M KOH onto TSKgel DNA-NPR column (4.6 × 75 mm). Elution was performed using a 20 min linear gradient between 0 and 1 M KCl in 0.1 M KOH at a flow rate of 0.6 ml/min.

mass corresponds with 5′-CCCCCCCCCCCCA-3′, to which 4 more C-bases have been added. No intermediate products derived from extension of 5′-CCCCCCCCCCCCA-3′ by 1, 2 or 3 nt were detected. This suggests that the rate-limiting step of the reaction is associated with template formation by the enzyme, rather than the addition of nucleotides to the primer. As seen in Figure 8 (red curve), 10 min incubation of 5 µM oligonucleotide with 10 µg/ml Klenow exo$^-$ at 37°C results in the conversion of ∼56% of the oligonucleotide to the product. Based on these data, a turnover number of 5.6 min^{-1} was calculated for the enzyme in reaction to the oligonucleotide extension. Experiments similar to those described above, were performed on 5′-GGTGGGGGGGGGA-3′, 5′-GGGTGGGGGGGGA-3′, and on 5′-GGGGGTGGGGGGA-3′ annealed with 5′-CCC-CCCCCCCCA-3′. Products of all the above template-primer extensions were analyzed by HPLC and mass spectrometry as

described in Figure 8. Data of the analysis (see Table 3) show that the amount of bases added to the primer is equal to the amount of G bases separating T from the 5′ end in the template strand. Turnover of the enzyme in the reaction of strand extension drops with a number of G nucleotides separating T from the 5′ end. This proves that an overall rate of extension is controlled by the rate of template-primer formation, and depends on a number of base pairs perturbed during the template formation. The dependence is neither linear nor exponential; the turnover number is reduced smoothly with an increasing number of bases in the range from 1 to 3; further increase in the number results in sharp reduction of the extension rate (see Table 3).

DISCUSSION

Poly(dG)–poly(dC), being a regular polymer with high G-base content, provides good conditions for charge migration, making the polymer a promising candidate for use in nanoelectronics. However, we have shown that the commercial preparations of poly(dG)–poly(dC) have a number of disadvantages that should be taken into account by researchers using the preparation in their work. The molecules composing the preparation have a tendency to form high-molecular weight aggregates, which do not enter agarose gels, and behave as a high-molecular weight species on size-exclusion columns. These structures are stable and do not dissociate while heating the preparation for 30 min at 70°C. A small fraction of the molecules, which enters the gel after the heating, shows a broad distribution of the molecule lengths (see Figure 1). We have shown (see Figure 2) that the average length of the C-homopolymers composing the preparation is about five times longer than that of the corresponding G-homopolymers. The preparation, in addition to long (more than thousand bases) C-homopolymers, contains much shorter (tens of bases) poly(dG) and poly(dC) fragments. These fragments were eluted as a small peak from the size-exclusion column in total volume (see Figure 2, dashed curve). The HPLC and the electrophoretic analysis led us to suggest that commercial preparations of poly(dG)–poly(dC) composed of long C-homopolymers and shorter G-fragments are not covalently connected one to another. Overhangs at the ends of poly(dG)–poly(dC) can thus exist as a result of improper matching of the G- and C-homopolymers. Formation of high-molecular weight aggregates in solution of the commercial polymer (see Figure 1, lanes 2 and 3) might be the result of overhangs-assisted interaction between the DNA molecules.

A method of poly(dG)–poly(dC) synthesis described here yields uniform polymers, which lack the above disadvantages. The synthesized polymer moves as a single band on electrophoresis (see Figure 1, lane 4), comprises equal amounts of dG and dC nucleotides (see Figure 4 and Table 1), and is composed of dG- and dC-homopolymers having equal lengths (see Figure 2, solid curve). The polymer is efficiently digested by DNase, and is stained with ethidium bromide. The polymer, in contrast to that obtained from Sigma, can thus be considered as a double-stranded poly(dG)–poly(dC) comprising two consecutive G- and C-homopolymer strands of equal length. The method enables the production of poly(dG)–poly(dC) of well-defined length and narrow size distribution of the molecules;

polymers varying in size from tens to ten thousand base pairs can be manufactured.

We have shown that covalent modification of the 5′ ends with thiol-groups has no effect on the ability of $(dC)_{12}$–$(dG)_{12}$ to prime the synthesis (see Table 2). Thiols and disulfides are known to interact specifically with gold (27,28). Introduction of SH-groups at the ends of DNA was used to anchor the DNA fragments to flat gold surfaces (29). When thiol groups have been introduced at the 5′ ends of $(dG)_{12}$–$(dC)_{12}$ by appropriate modification, poly(dG)–poly(dC) resulting from the oligonucleotide extension was easily absorbed on gold surfaces, as evident from a data of atomic force microscopy (data not shown). The ability to introduce SH-groups into the 5′ ends provides a tool for the selective attachment of long poly(dG)–poly(dC) polymers to gold surfaces and gold nanoelectrodes. This property is especially useful for application of the polymer in nanoelectronics.

It has been earlier proposed (18,30,31) that the synthesis of simple repeating sequences proceeds via slippage of the strands composing template-primers. Direct demonstration of strands, which slide during polymerization has, to the best of our knowledge, never been reported so far. Ability to attach fluorescent dyes to the 5′ ends of $(dG)_{12}$–$(dC)_{12}$ enabled us to directly monitor the strands sliding during template-primer extension by polymerase by using FRET. Growth of poly(dG)–poly(dC) was followed in time by a look at the emission of Flu attached to the growing polymer. We have clearly demonstrated (see Figures 5 and 6) that the distance between 5′ ends of double-labeled Flu-$(dG)_{12}$–$(dC)_{12}$-TAMRA oligonucleotide (fluorescence of Flu) increases during the synthesis. The above results suggest that the labeled 5′ ends of template-primer move in opposite directions during the extension process, leading to the formation of complete double-stranded poly(dG)–poly(dC) with Flu and TAMRA on its 5′ ends.

A molecular mechanism of strands slippage during the synthesis is not well established. To explain slippage, two models can be considered. In one scenario, one of the strands composing poly(dG)–poly(dC) slides on the other, providing template regions on both the 3′ ends of the polymer which, when filled in by the polymerase, increased the strand's length. A number of successive slippage and replication cycles then leads to a long double-stranded polymer. Sliding of the strand should thus involve complete breakage and reformation of all G–C base pairs of the entire polymer. The activation energy of the process of this reaction is proportional to a number of bases composing poly(dG)–poly(dC) and, if the proceedings are in accordance with the above scenario, the rate of the polymer growth should drop exponentially with a number of bases composing the polymer. Our experiments, however, show that the rate of the synthesis is largely independent of the length of the DNA fragments being synthesized (see Figure 3). In the second scenario, the enzyme binds to the 3′ end of DNA, shifts the end-nucleotide on the 3′ end of the polymer in 5′-direction and generates a short, single-stranded template and a loop *de novo*. Formation of a loop is driven by the interaction of DNA with polymerase and is associated with the melting and rearrangement of hydrogen bonds at the end of poly(dG)–poly(dC). Loop migration through the DNA results in the formation of a template region on its opposite end; filling the template by polymerase finalizes a single extension
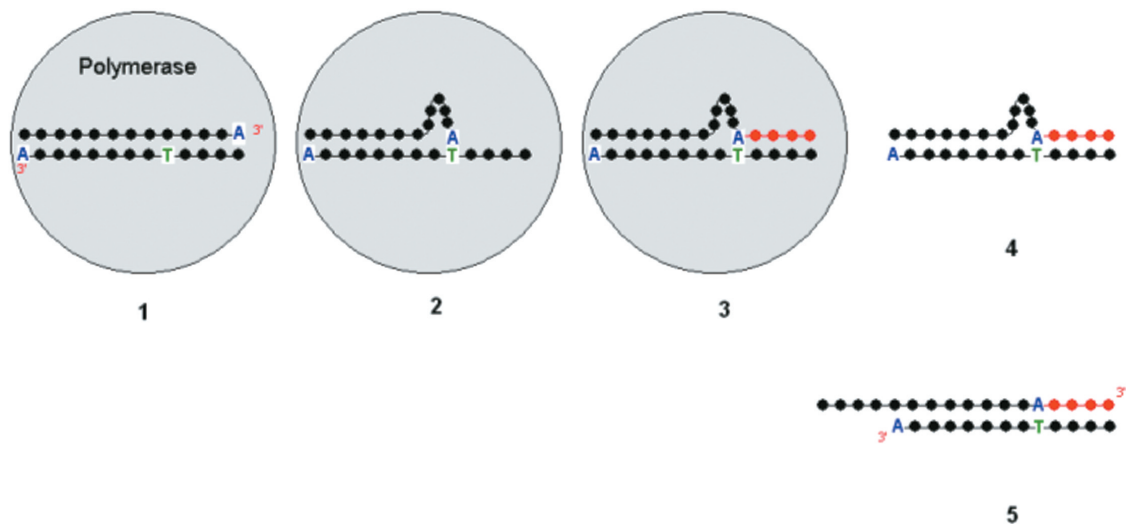
Figure 9. Model for 5′-CCCCCCCCCCCCCA-3′–5′-GGGGTGGGGGGGGA-3′ extension. The figure depicts the assumed events during the extension of double-stranded 5′-CCCCCCCCCCCCCA-3′–5′-GGGGTGGGGGGGGA-3′ oligonucleotide. Polymerase binds the oligonucleotide (**1**) and shifts A-nucleotide at the 3′ end of 5′-CCCCCCCCCCCCCA-3′ until it is paired with T. A single-stranded template-primer fragment and a loop *de novo* are then formed as a result of the 3′ end slippage (**2**). The primer strand is synthesized complementary to the template sequence; residues incorporated into the primer are marked in red (**3**). The enzyme–DNA complex dissociates (**4**) and a loop relaxes into a structure with overhang at the 5′ end (**5**). The overhang cannot be used as a template for Klenow exo⁻ due to inability to pair A-nucleotide at the 3′ end of the primer with either nucleotide in sequence of the template.

cycle. Loop formation requires pairing of nucleotide at the 3′ end of the primer strand with a complimentary nucleotide in the sequence of template strand in accord with the base-pairing rules. In the case of poly(dG)–poly(dC), a nucleotide to which the 3′ end one is paired, is located next to the 5′ end one in the sequence. We have shown that an elementary step of poly(dG)–poly(dC) extension includes the addition of one base to each strand of the polymer, thus, proving the above suggestion. If proper pairing of the 3′ end nucleotide is not present, the synthesis does not take place. We showed that, if the 3′ end nucleotides in poly(dG) and poly(dC) strands were substituted for A one, the polymer did not grow (see Table 2). Introduction of T-nucleotide into the complementary strand to allow pairing with the A-nucleotide resulted in restoration of the synthesis. Analysis of the products of 5′-CCCCCCCCCCCCCA-3′–5′-GGGGTGGGGGGGGA-3′ replication by Klenow exo⁻ in the presence of dGTP and dCTP showed, that four C-nucleotides were added to the 5′-CCCCCCCCCCCCCA-3′-strand; 5′-GGGGTGGGGGGGGA-3′-strand was not expanded. These data can be explained (see Figure 9) by the assumption that the enzyme binds the oligonucleotide and shifts the A-base at the 3′ end of 5′-CCC-CCCCCCCCA-3′ until it is paired with the T-nucleotide of the 5′-GGGGTGGGGGGGGA-3′-template strand. A single-stranded template and a loop *de novo* are then formed. The template is subsequently filled by polymerase to complete the extension cycle. An overall rate of strand extension is controlled by the rate of template-primer formation. Once formed, a template is rapidly filled by polymerase before the enzyme–DNA complex dissociates. This conclusion is supported by the following experimental observations: (i) no intermediate products were observed with a number of nucleotides added to 5′-CCCCCCCCCCCCCA-3′, which is less than that separating the T-nucleotide from the 5′ end of

the complementary strand; and (ii) the rate of 5′-CCCCCCCC-CCCCA-3′ extension decreases with an increase in the distance separating the T-nucleotide from the 5′ end of the template. The oligonucleotide dissociates from the complex with the enzyme after the template has been filled and a loop relaxes into a structure with an overhang at the 5′ end. The overhang cannot be used as a template for Klenow exo⁻. The later is due to the absence of T-nucleotide in the sequence of template with which A-nucleotide at the 3′ end of the primer could be paired; proper pairing of the 3′ end of the primer strand seems to be strictly required for initiation of the synthesis. The rate of extension depends on the number of bases that composes the proposed loop. We have shown that the rate of extension is relatively high for a number of bases between one and three. Only a slight decrease in the extension rate with an increasing number of bases was observed (see Table 3). A further increase in the number of bases resulted in a sharp reduction of the extension rate. This is probably due to the high activation energy of the template formation, which strongly limits the rate of extension if the number of bases exceeded three.

The rate of polymer growth is independent of the length of the fragments being synthesized. We have shown that poly(dG)–poly(dC) as long as 10 kb, continues to grow at the rate equal to 50 bp/min. If loop migration through the DNA takes place while it is elongated, the loop should skip through 3 μm (length of the extended 10 kb DNA) distance in seconds. Movement of a loop over long molecular distances most probably proceeds through a sequence of elementary transfer steps, each including the movement of a loop one base pair towards an opposite end of the polymer. This movement includes the opening of a G–C pair and thus is determined by base pairs opening dynamics. In general, G–C base pair lifetimes have been found to be approximately

equal to 10–20 ms (32–34); however, in tracts, G–C have unusually rapid base pair dynamics (35), leading to a much higher base pair dissociation constant. Fast rate of poly(dG)–poly(dC) replication can alternatively be explained by the assumption that multiple loops migrate simultaneously in opposite directions through DNA. Such loops can, in principle, be structurally accommodated in a DNA helix (36).

ACKNOWLEDGEMENTS

REFERENCES

1. Kornberg,A. (1974) DNA polymerase of *E.coli*. In *DNA Synthesis*. W. J. Freeman and Co., San Francisco, CA, 103.
2. Schachman,H.K., Adler,J., Radding,C.M., Lehman,I.R. and Kornberg,A. (1960) Enzymatic synthesis of deoxyribonucleic acid. VII. Synthesis of a polymer of deoxyadenylate and deoxythymidylate. *J. Biol. Chem.*, **235**, 3242–3249.
3. Radding,C.M., Josse,J. and Kornberg,A. (1962) Enzymatic synthesis of deoxyribonucleic acid. XII. A polymer of deoxyguanylate and deoxycytidylate. *J. Biol. Chem.*, **237**, 2869–2876.
4. Inman,R.B. and Baldwin,R.L. (1964) Helix-random coil transitions in DNA homopolymer pairs. *J. Mol. Biol.*, **41**, 452–469.
5. Burd,J.F. and Wells,R.D. (1970) Effect of incubation conditions on the nucleotide sequence of DNA products of unprimed DNA polymerase reactions. *J. Mol. Biol.*, **53**, 435–459.
6. Grant,R.C., Harwood,S.J. and Wells,R.D. (1972) The synthesis and characterization of poly d(I-C) poly d(I-C). *J. Am. Chem. Soc.*, **90**, 4474–4476.
7. Grant,R.C., Kodama,M. and Wells,R.D. (1972) Enzymatic and physical studies on (dI–dC)$_n$-(dI–dC)$_n$ and (dG–dC)$_n$-(dG–dC)$_n$. *Biochemistry*, **11**, 805–815.
8. Wells,R.D., Larson,J.E., Grant,R.C., Shortle,B.E. and Cantor,C.R. (1970) Physicochemical studies on polydeoxyribonucleotides containing defined repeating nucleotide sequences. *J. Mol. Biol.*, **54**, 465–497.
9. Green,G. and Mahler,H.R. (1971) Conformational changes of deoxyribonucleic acid and polydeoxynucleotides in water and ethylene glycol. *Biochemistry*, **10**, 2200–2216.
10. Gray,D.M. and Bollum,F.J. (1974) A circular dichroism study of poly dG, poly dC, and poly dG:dC. *Biopolymers*, **13**, 2087–2102.
11. Porath,D., Bezryadin,A., de Vries,S. and Dekker,C. (2000) Direct measurement of electrical transport through DNA molecules. *Nature*, **403**, 635–638.
12. Hwang,J.S.K., Kong,J., Ahn,D.G., Lee,S., Ahn,D.J.S. and Hwang,W. (2002) Electrical transport through 60 base pairs of poly(dG)-poly(dC) DNA molecules. *Appl. Phys. Lett.*, **81**, 1134–1136.
13. Hennig,D., Starikov,E.B., Archilla,J.F.R. and Palmero,F. (2004) Charge transport in poly(dG)-poly(dC) and poly(dA)-poly(dT) DNA polymers. *J. Biol. Phys.*, **30**, 227–238.
14. Lee,H.-Y., Tanaka,H., Otsuka,Y., Yoo,K.-H., Lee,J.-O. and Kawai,T. (2002) Control of electrical conduction in DNA using oxygen hole doping. *App. Phys. Lett.*, **80**, 1670–1672.
15. Yoo,K.-H., Ha,D.H., Lee,J.-O., Park,J.W., Kim,J., Kim,J.J., Lee,H.-Y., Kawai,T. and Choi,H.-Y. (2001) Electrical conduction through Poly(dA)–Poly(dT) and Poly(dG)–Poly(dC) DNA molecules. *Phys. Rev. Lett.*, **87**, 198102.
16. Sjoback,R., Nygren,J. and Kubista,M. (1998) Characterization of fluorescein-oligonucleotide conjugates and measurement of local electrostatic potential. *Biopolymers*, **46**, 445–453.
17. Huber,C.G. and Krojete,A. (2000) Comparison of direct infusion and on-line liquid chromatography/electrospray ionization mass spectrometry for the analysis of nucleic acids. *J. Mass Spectrom.*, **35**, 870–877.
18. Karthikeyan,G., Chary,K.V. and Rao,B.J. (1999) Fold-back structures at the distal end influence DNA slippage at the proximal end during mononucleotide repeat expansions. *Nucleic Acids Res.*, **27**, 3851–3858.
19. Thiele,D., Marck,C., Schneider,C. and Guschlbauer,W. (1978) Protonated polynucleotides structures–23. The acid–base hysteresis of poly(dG) poly(dC). *Nucleic Acids Res.*, **5**, 1997–2012.
20. Marck,C., Thiele,D., Schneider,C. and Guschlbauer,W. (1978) Protonated polynucleotides structures–22. CD study of the acid–base titration of poly(dG) poly(dC). *Nucleic Acids Res.*, **5**, 1979–1996.
21. Davis,J.T. (2004) G-quartets 40 years later: from 5′-GMP to molecular biology and supramolecular chemistry. *Angew. Chem. Int.*, **43**, 668–698.
22. Simonsson,T. (2001) G-quadruplex DNA structures––variations on a theme. *Biol. Chem.*, **382**, 621–628.
23. Clegg,R.M. (1992) Fluorescence resonance energy transfer and nucleic acids. *Methods Enzymol.*, **211**, 353–388.
24. Lilley,D.M. and Wilson,T.J. (2000) Fluorescence resonance energy transfer as a structural tool for nucleic acids. *Curr. Opin. Chem. Biol.*, **4**, 507–517.
25. Stryer,L. (1978) Fluorescence energy transfer as a spectroscopic ruler. *Annu. Rev. Biochem.*, **47**, 819–846.
26. Wu,P. and Brand,L. (1994) Resonance energy transfer: methods and applications. *Anal. Biochem.*, **218**, 1–13.
27. Nuzzo,R.G. and Allara,D.L. (1983) Adsorption of bifunctional organic disulfides on gold surfaces. *J. Am. Chem. Soc.*, **105**, 4481–4483.
28. Sellers,H., Ulman,A., Shnidman,Y. and Eilerss,J.E. (1993) Structure and binding of alkanethiolates on gold and silver surfaces: implications for self-assembled monolayers. *J. Am. Chem. Soc.*, **115**, 9389–9401.
29. Hegner,M., Wagner,P. and Semenza,G. (1993) Immobilizing DNA on gold via thiol modification for atomic force microscopy imaging in buffer solutions. *FEBS Lett.*, **336**, 452–456.
30. Schlottererand,C. and Tautz,D. (1992) Slippage synthesis of simple sequence DNA. *Nucleic Acids Res.*, **20**, 211–215.
31. Ji,J., Clegg,N.J., Peterson,K.R., Jackson,A.L., Laird,C.D. and Loeb,L.A. (1996) *In vitro* expansion of GGC:GCC repeats: identification of the preferred strand of expansion. *Nucleic Acid Res.*, **24**, 2835–2840.
32. Kochoyan,M., Lancelot,G. and Leroy,J.L. (1988) Study of structure, base-pair opening kinetics and proton exchange mechanism of the d-(AATTGCAATT) self-complementary oligodeoxynucleotide in solution. *Nucleic Acids Res.*, **16**, 7685–7702.
33. Leroy,J.L., Charretier,E., Kochoyan,M. and Gueron,M. (1988) Evidence from base-pair kinetics for two types of adenine tract structures in solution: their relation to DNA curvature. *Biochemistry*, **27**, 8894–8898.
34. Folta-Stogniew,E. and Russu,I.M. (1994) Sequence dependence of base-pair opening in a DNA dodecamer containing the CACA/GTGT sequence motif. *Biochemistry*, **33**, 11016–11024.
35. Dornberger,U., Leijon,M. and Fritzsche,H. (1999) High base pair opening rates in tracts of GC base pairs. *J. Biol. Chem.*, **274**, 6957–6962.
36. Fresco,J.R. and Alberts,B.M. (1960) The accommodation of noncomplementary bases in helical polyribonucleotides and deoxyribonucleic acids. *Proc. Natl Acad. Sci. USA*, **46**, 311–321.